34th Annual International Conference of the IEEE EMBS
San Diego, California USA, 28 August - 1 September, 2012

Brain State Evolution During Seizure and Under Anesthesia: A Network-Based Analysis of Stereotaxic EEG Activity in Drug-Resistant Epilepsy Patients

Robert Yaffe, Sam Burns, John Gale, Hyun-Joo Park, Juan Bulacio,
Jorge Gonzalez-Martinez, and Sridevi V. Sarma, *Member, IEEE*

Abstract— **Epilepsy is a neurological condition with a prevalence of 1%, and 14-34% have medically refractory epilepsy (MRE). Seizures in focal MRE are generated by a single epileptogenic zone (or focus), thus there is potentially a curative procedure - surgical resection. This procedure depends significantly on correct identification of the focus, which is often uncertain in clinical practice. In this study, we analyzed intracranial stereotaxic EEG (sEEG) data recorded in two human patients with drug-resistant epilepsy prior to undergoing resection surgery. We view the sEEG data as samples from the brain network and hypothesize that seizure foci can be identified based on their network connectivity during seizure. Specifically, we computed a time sequence of connectivity matrices from EEG recordings that represent network structure over time. For each patient, connectivity between electrodes was measured using the coherence in a given frequency band. Matrix structure was analyzed using singular value decomposition and the leading singular vector was used to estimate each electrode's time dependent centrality (importance to the network's connectivity). Our preliminary study suggests that seizure foci may be the most weakly connected regions in the brain during the beginning of a seizure and the most strongly connected regions towards the end of a seizure. Additionally, in one of the patients analyzed, the network connectivity under anesthesia highlights seizure foci. Ultimately, network centrality computed from sEEG activity may be used to develop an automated, reliable, and computationally efficient algorithm for identifying seizure foci.**

I. INTRODUCTION

Epilepsy affects 50 million people worldwide [1], and 30% remain drug-resistant [2]. This has increased interest in both chronic and responsive or closed-loop neurostimulation [3], which is most effective when administered at or near the seizure foci (brain region causing or facilitating seizures). Precise foci localization from intracranial EEG (iEEG) or stereotaxic EEG (sEEG) recordings is therefore critical for closed-loop intervention, but remains a challenging problem. The identification of seizure foci is traditionally performed by epileptologists who evaluate EEG recordings. From these recordings, the onset of seizures and the nature of interictal epileptiform spikes are inspected to determine the location of the seizure focus or foci [9]. Depending on the location of identified foci, clinicians decide whether or not resecting this area of the brain is likely to relieve the patient of his/her seizure activity. The manual inspection of long extraoperative recordings (days to weeks) by epileptologists is very time consuming and there is a need for a computational means of determining the location of seizure foci. Furthermore, it has been shown that in many cases seizures spread through the brain so rapidly that visual analysis cannot discern the seizure focus in patients that had MRI identified focal lesions [10].

Univariate efforts to algorithmically estimate seizure focus location have examined the propagation of interictal spikes and their morphology [4]. These methods do not examine the relationship between channels and do not directly yield information regarding the flow of activity between brain regions [8]. The concept that a seizure is a network phenomenon that involves the interaction of different regions has motivated work on bivariate measures of the dependence of signals recorded at different electrodes for focus localization. These measures include linear and cross-correlations [14], direct transfer functions based on Granger causality [8], phase synchrony using the Hilbert transform [13], information theory [12], Fourier analysis [6] and nonlinear interactions [5]. These studies have examined the patterns of pair-wise interactions between electrodes and typically identify the seizure focus as the location that shows the greatest amount of dependence with other electrode sites.

Recently, there has been research on analyzing brain activity as a multivariate problem through the application of graph theory and network analysis methods from sociology and physics [7]. Here, the collection of pair-wise interactions are organized in a graph and analyzed simultaneously. Some studies use metrics derived from social networks that commonly focus on summary statistics of the time dependence of the brains connectivity during interictal and seizure periods [11]. These studies have found that the onset of seizure commonly corresponds to fluctuating values of network connectivity. In relation to the seizure focus; there have been some results that identify the electrode with the greatest betweenness centrality to the focus [15].

Here, we further develop the network analysis of sEEG data during both interictal and seizure states by examining the eigenvectors of the network connectivity graph. But rather than treat the eigenvectors only as an abstract representation of the brain state, we exploit the property that

R. Yaffe, S. Burns, and S. V. Sarma are with the Department of Biomedical Engineering, Johns Hopkins University, Baltimore, MD 21218 USA (corresponding author: R. Yaffe; e-mail: yaffer@jhu.edu).

J. Bulacio, J. Gonzalez-Martinez, and H. Park are with the Epilepsy Center, Cleveland Clinic, Cleveland, OH 44195 USA

J. Gale is with the Department of Neurosciences, Cleveland Clinic, Cleveland, OH 44195 USA

978-1-4577-1787-1/12/$26.00 ©2012 IEEE

they can be related to the immediate features of the network through their interpretation as measures of the networks eigenvector centrality. We propose to use this technique as a means of identifying the seizure focus by examining the connectivity of the entire network both during seizure and interictal periods. This method has the advantage of incorporating information from all electrodes rather than pair-wise techniques and is computationally more efficient than social network measures.

II. Methods

A. Experimental Data

We use data collected from two patients (previously monitored with stereotaxic depth electrodes as part of their presurgical evaluation at the Cleveland Clinic Epilepsy Center) in this study. Recordings were taken while the patients were under anesthesia as well as while they were being monitored in the epilepsy monitoring unit. The decisions regarding the need for invasive monitoring and the placement of depth electrodes were made independently of this project and solely based on clinical necessity. Acquisition of data for research purposes was done with no impact on the clinical objectives of the patient stay. The data recorded for clinical purposes are stored in a database compliant with HIPAA regulations.

The two patients analyzed in this study had stereotaxic depth electrodes implanted. Table 1 summarizes patient information for the two subjects used in this study. Fig. 1 shows a diagram of subject 005's brain and the placement of the depth electrodes. Each depth electrode had approximately 10 recording contacts along the length of the electrode. The recording contacts were numerically labeled going from deepest to most superficial. For example, if electrode B had 10 recording sites, then B1 would be the deepest contact and B10 would be the most superficial contact.

TABLE I
Patient Information

Subject	Age	Sex	Handedness	Seizure Location
002	38	F	Right	Right Temporal Lobe
005	27	F	Right	Right Mesial Temporal Lobe

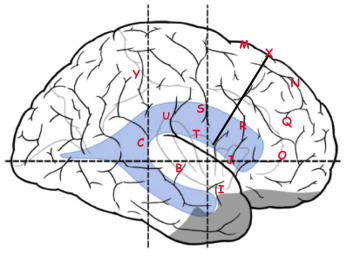

Fig. 1. Diagram of electrode placement for subject 005.

B. Data Analysis

1) Determining the Frequency Band for Each Patient: The frequency band for each patient was determined by choosing the frequency band that showed the greatest change in the ranked centrality values of the network near seizure onset.

2) Computing Network Connectivity over Time: Coherence between two channels was computed as a metric of the connectivity between those two channels. A sliding 5-second window with a displacement of 1-second, was used to calculate coherence values for 5-second blocks of data. Within each 5-second window, a 1-second sliding window was used to compute an average coherence over the 5-second window. The 1-second sliding window had a displacement of 0.25 seconds. For each 1-second window, the signal from each channel was preprocessed by multiplication by a Hamming window. For a given 1-second window, the preprocessed signal from channel i will be referred to as S_i. Then, for each channel, the autospectral density of S_i was computed. Autospectral density of S_i was defined as $|\mathcal{F}(S_i)|$, where $\mathcal{F}$ is the discrete Fourier transform. For each pair of channels, the cross-spectral density of the two preprocessed channels was computed. Cross-spectral density of S_i and S_j was defined as the point-wise multiplication of $\mathcal{F}(S_i)$ and $\mathcal{F}(S_j)$. Then, the average of the cross-spectral density values and the average of the autospectral density values were taken across all of the 1-second windows within a 5-second window. For each 5-second window, this yielded an average cross-spectral density for each pair of channels (G_{xy}) and an average autospectral density for each channel (G_{xx}). Then, the coherence between two channels x and y, was calculated as $C_{xy} = \frac{|G_{xy}|^2}{G_{xx}G_{yy}}$. For every 5-second window, an adjacency matrix, A, is constructed, where each entry $A_{ij} = C_{ij}$.

3) Computing Eigenvector Centrality over Time: The centrality of a node is defined as the weighted sum of the centralities of its neighbors. The centrality of node i, $x(i)$, is mathematically defined as

$$x(i) = \sum_{j=1}^{n} A_{ij}x(j)$$

where A is the connectivity matrix of the network. Written in matrix notation, this becomes $\mathbf{x} = A\mathbf{x}$. It can be shown that $\mathbf{x}$ is the eigenvector corresponding to the largest eigenvalue in the solution to the eigenvalue problem $A\mathbf{v} = \lambda\mathbf{v}$.

At each point in time, singular vector decomposition is performed on A. Due to the way A is constructed, A is always a square symmetric matrix. Therefore, the first singular vector of A is equal to the eigenvector of A corresponding to the largest eigenvalue. Thus, the first singular vector is the centrality vector of the network. The first singular vector of A is computed at every time point and the centralities of the nodes in the network can be tracked over time. The centrality vectors are now ranked and each element in the vector is assigned the value of its rank. For example, the node with the lowest centrality is reassigned to 1; the node with second lowest centrality is reassigned to 2, and so on.

4) Determining the Brain States: Clustering is performed on the ranked centrality vectors to identify different brain

states. The connectivity of the brain changes over time and over the course of a seizure and the centrality vectors capture these changes. K-means clustering was used to cluster the ranked centrality vectors. Once the ranked centrality vectors are clustered into discrete states, then a state transition diagram is drawn for each seizure and the state transition probabilities can be estimated.

III. Results

All the results will be shown for subject 005. The same steps were performed for subject 002.

A. Determining the Frequency Band for Each Patient

For both patients analyzed, the beta frequency band (13-25Hz) showed the most modulation in the network connectivity near seizure onset. For this reason, beta was chosen as the frequency band to analyze in both patients.

B. Computing Network Connectivity over Time

Coherence in the beta band was computed between each pair of nodes for every 5-second window of data, using a 5-second sliding window with a displacement of 1-second. For each 5-second window, the coherence values were stored in a connectivity matrix A.

C. Computing Eigenvector Centrality over Time

The first singular vector of A was computed for each 5-second window. The bottom row of figs. 2 and 3 show plots of the first singular vectors over time for subject 005. These plots show snapshots of the data around the patient's seizures as well as a snapshot of inter-ictal data and a snapshot of anesthesia data.

D. Determining the Brain States

By looking at the bottom plots in Figs. 2 and 3, one can visually identify distinct states. These states were formally identified by k-means clustering, where k is the number of clusters. For subject 005, k-means clustering was run on just the seizure snapshot data (100 seconds before each seizure, each seizure, and 100 seconds after each seizure) with k=11. Then, k-means clustering was run on all the inter-ictal data with k=2. One of the inter-ictal cluster's centroid matched very closely to the centroid of a cluster identified by the clustering of the seizure snapshot data, so these two clusters were merged by taking the point by point average of the two centroids. Then, k-means clustering was run on all of the anesthesia data with k=2. This yielded a total of 14 clusters for subject 005, with each cluster representing a discrete brain state. Using these 14 states, state membership was plotted over time. These plots can be seen in the top plots of Fig. 2 and Fig. 3.

The state transitions in a simplified diagrammatic format are shown in Fig. 4. Six seizure states were identified and they are labeled S1 through S6. Note the consistency amongst the beginning of each seizure. Each seizure enters into S1 then goes to S2.

For subject 002, k-means clustering was run on the seizure snapshot data with k=8. The same procedure was followed

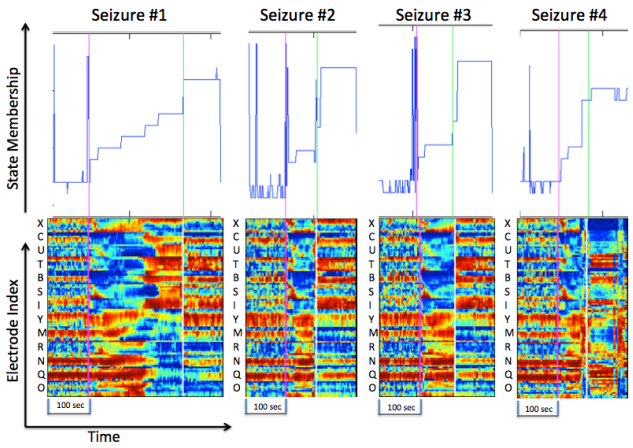

Fig. 2. Top: Cluster membership over time for seizure snapshots. Bottom: First singular vectors over time. X-axis is time. Y-axis is electrode index. Color indicates ranked centrality. The letters along the Y-axis are the electrode labels that correspond to the electrode labels in Fig. 1. The pink line indicates seizure onset and the white line indicates seizure end. The plots show 100 seconds before seizure, the length of the seizure, and 100 seconds after seizure.

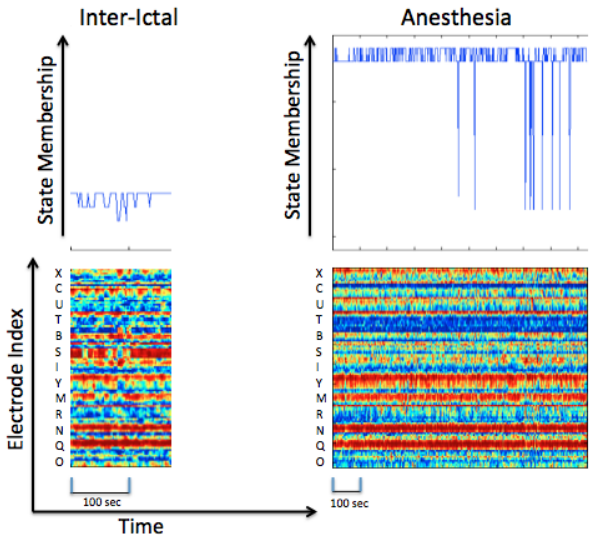

Fig. 3. Cluster membership over time for inter-ictal snapshot and anesthesia data. Bottom: First singular vectors over time. X-axis is time. Y-axis is electrode index. Color indicates ranked centrality. The letters along the Y-axis are the electrode labels that correspond to the electrode labels in Fig. 1.

and five seizure clusters were identified, S1 through S5. It was again found that all seizures entered into S1 and then progressed to S2. Note that these states are different from the states identified in subject 005 even though the same notation is used for both subjects.

E. Comparing Foci Centrality to Brain State

For subject 005, recording sites B1-3 and C1-2 were clinically identified as the seizure foci. The centrality of the foci nodes were examined for each state. For subject 005, the foci had low centralities ("foci cold") in states S1 and S2 and high centralities ("foci hot") in state S4. This is illustrated by the colors in Fig. 4. Fig. 5 shows the centrality values for

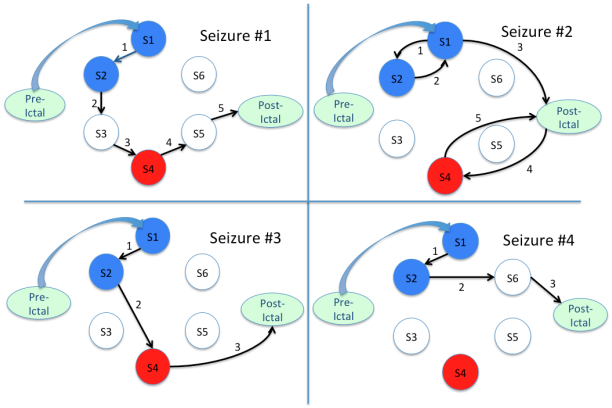

Fig. 4. State transition diagrams for subject 005's four seizures. Blue indicates a "foci cold" state and red indicates a "foci hot" state.

each recording site for states S1, S4 and an anesthesia state. The letters at the top of the plots indicate the electrode. The recording sites within an electrode block go in increasing order from left to right. For example, in the block marked B, B1 is the leftmost point in that block. In S1, the foci (B1-3 and C1-2) are clearly the least central nodes in the network. In S4, the clinically identified foci have high centralities but there are other nodes that have equally high centralities. The electrodes that also have high centralities in this state are T and I, which are nearby to B and C as you can see from Fig. 1. In the anesthesia state, the foci nodes also are the least central. For this patient, the foci nodes can be identified from the anesthesia data alone.

For subject 002, recording sites A2 and E2 were clinically identified as the seizure foci. Again, the centrality of the foci were examined for each state. It was again found that the foci had low centralities in states S1 and S2 and high centralities in state S4. The centralities of the foci for this patient did not clearly identify them as the foci. Additionally, the anesthesia data for this patient did not seem to highlight the foci in a meaningful way.

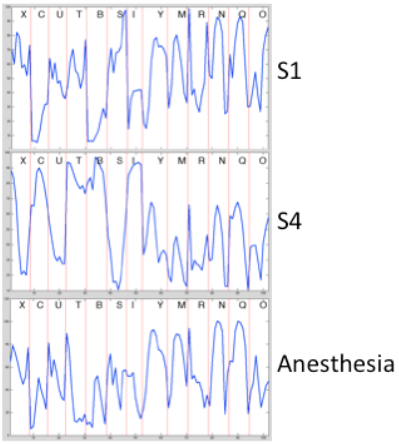

Fig. 5. Centralities of nodes in S1, S4, and anesthesia state for subject 005.

IV. CONCLUSIONS

From the preliminary analysis of this data, it appears that there are discrete brain states characterized by the connectivity of the brain. There are consistent brain states seen in the beginnings of seizures across seizures for a given patient and the foci have low centrality in these states. Towards the middle and the end of seizures, the foci have high centrality. In one patient, the connectivity of the anesthesia state highlighted the foci, and in one patient, it did not. Ideally, a technique will be developed to perform seizure foci localization from anesthesia recordings alone. This would allow neurosurgeons to identify seizure foci much more quickly and could greatly reduce the amount of time patients need to be monitored in the epilepsy monitoring unit.

ACKNOWLEDGMENT

S. V. Sarma was supported by the Burroughs Wellcome Fund CASI Award 1007274 and the National Science Foundation CAREER Award 1055560.

REFERENCES

[1] de Boer HM, Mula M, Sander JW (2008) The global burden and stigma of epilepsy. Epilepsy Behav. 12:540-546.
[2] Schmidt D (2009) Drug treatment of epilepsy: options and limitations. Epilepsy Behav. 15:56-65.
[3] Jobst BC, Darcey TM, Thadani VM, Roberts DW (2010) Brain stimulation for the treatment of epilepsy. Epilepsia 51:S88-S92.
[4] Alarcon G, Garcia Seoane J J, Binnie C D, Martin Miguel M C, Juler J, Polkey C E, Elwes R D C, Ortiz Blasco J M (1997) Origin and propagation of interictal discharges in the acute electrocorticogram Implications for pathophysiology and surgical treatment of temporal lobe epilepsy. Brain, 120:2259-2282.
[5] Andrzejak R G, Chicharro D, Lehnertz K, Mormann F (2011) Using bivariate signal analysis to characterize the epileptic focus: The benefit of surrogates. Phys. Rev. E, 83:046203.
[6] Ben-Jacob E, Doron I, Gazit T, Rephaeli E, Sagher O, Towle V L (2007b) Mapping and assessment of epileptogenic foci using frequency-entropy templates. Phys. Rev. E, 76:051903.
[7] Bullmore E, Sporns O (2009) Complex brain networks: graph theoretical analysis of structural and functional systems. Nat Rev. Neurosci., 10:186-198.
[8] Franaszczuk P J, Bergey G K (1998) Application of the directed transfer function method to mesial and lateral onset temporal lobe seizures. Brain Topogr., 11(1):13-21.
[9] Jung W Y, Pacia S V, Devinsky O (1999) Neocortical temporal lobe epilepsy: intracranial EEG features and surgical outcome. J. Clin. Neurophysiol., 16(5):419-428.
[10] Matsuoka L, Spencer S (1993) Seizure localization using subdural grid electrodes. Epilepsia, 34(6):8.
[11] Ponten S C, Bartolomei F, Stam C J (2007) Small-world networks and epilepsy: Graph theoretical analysis of intracerebrally recorded mesial temporal lobe seizures. Clin. Neurophys., 118:918-927.
[12] Sabesan S, Good L B, Tsaklis K S, Spanias A, Treiman D M, Iasemidis L D (2009) Information flow and application to epileptogenic focus localization from intracranial EEG. IEEE Trans. Neural Sys. Rehab. Eng., 17(3):244-253.
[13] Schevon C A, Cappell J, Emerson R, Isler J, Grieve P, Goodman R, Mckhann G, Weiner H, Doyle W, Kuzniecky R, Devinsky O, Gilliam F (2007) Cortical abnormalities in epilepsy revealed by local EEG synchrony. NeuroImage, 35:140:148.
[14] Warren C P, Hu S, Stead M, Brinkmann B H, Bower M R, Worrell G A (2010) Synchrony in normal and focal epileptic brain: the seizure onset zone is functionally disconnected. J. Neurophysiol., 104:3530-3539.
[15] Wilke C, Worrell G, He B (2011) Graph analysis of epileptogenic networks in human partial epilepsy. Epilepsia, 52(1):84-93.